Journal of Volcanology and Geothermal Research 200 (2011) 35–48

Contents lists available at ScienceDirect

Journal of Volcanology and Geothermal Research

journal homepage: www.elsevier.com/locate/jvolgeores

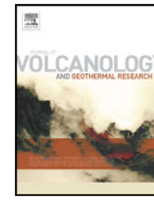

Infrasonic observations of the June 2009 Sarychev Peak eruption, Kuril Islands: Implications for infrasonic monitoring of remote explosive volcanism

Robin S. Matoza [a,*], Alexis Le Pichon [a], Julien Vergoz [a], Pascal Herry [a], Jean-Marie Lalande [a], Hee-il Lee [b], Il-Young Che [b], Alexander Rybin [c]

[a] CEA/DAM/DIF, F-91297 Arpajon, France
[b] Earthquake Research Center, Korea Institute of Geoscience and Mineral Resources, Korea
[c] Sakhalin Volcanic Eruptions Response Team, Institute of Marine Geology and Geophysics, Yuzhno-Sakhalinsk, Russia

ARTICLE INFO

Article history:
Received 1 June 2010
Accepted 25 November 2010
Available online 7 December 2010

Keywords:
explosive volcanism
infrasound atmospheric propagation
infrasound source location
volcano monitoring
volcano seismology

ABSTRACT

Sarychev Peak (SP), located on Ostrov Matua, Kurils, erupted explosively during 11–16 June 2009. Whereas remote seismic stations did not record the eruption, we report atmospheric infrasound (acoustic wave ~0.01–20 Hz) observations of the eruption at seven infrasound arrays located at ranges of ~640–6400 km from SP. The infrasound arrays consist of stations of the International Monitoring System global infrasound network and additional stations operated by the Korea Institute of Geoscience and Mineral Resources. Signals at the three closest recording stations IS44 (643 km, Petropavlovsk-Kamchatskiy, Kamchatka Krai, Russia), IS45 (1690 km, Ussuriysk, Russia), and IS30 (1774 km, Isumi, Japan) represent a detailed record of the explosion chronology that correlates well with an eruption chronology based on satellite data (TERRA, NOAA, MTSAT). The eruption chronology inferred from infrasound data has a higher temporal resolution than that obtained with satellite data. Atmosphere-corrected infrasonic source locations determined from backazimuth cross-bearings of first-arrivals have a mean centroid ~15 km from the true location of SP. Scatter in source locations of up to ~100 km result from currently unresolved details of atmospheric propagation and source complexity. We observe systematic time-variations in trace-velocity, backazimuth deviation, and signal frequency content at IS44. Preliminary investigation of atmospheric propagation from SP to IS44 indicates that these variations can be attributed to solar tide variability in the thermosphere. It is well known that additional information about active volcanic processes can be learned by deploying infrasonic sensors with seismometers at erupting volcanoes. This study further highlights the significant potential of infrasound arrays for monitoring volcanic regions such as the Kurils that have only sparse seismic network coverage.

1. Introduction

Sarychev Peak (SP), an andesitic stratovolcano (summit elevation 1446 m a.s.l.) on the northwest side of Ostrov Matua (Matua Island), Kurils (Fig. 1), erupted explosively during 11–16 June 2009. The eruption was first indicated by satellite data acquired on 11 June 2009 that showed a thermal anomaly and weak ash emissions (SVERT, 2009). Subsequently, at ~22:16 UT 12 June 2009, spectacular photographs of an eruption column issuing from SP were taken by astronauts aboard the International Space Station (ISS) (Fig. 1, inset). These photographs also captured ash dispersed at altitude from previous eruptions, and pyroclastic flows in the process of descending the mountain (Fig. 1, inset). Due to the remote location of the Kurils, ground-based observations are sparse. In particular, no seismic network was in place on SP at the time of the eruption and the eruption did not register on any remote seismic stations (e.g., seismic stations on Paramushir, Iturup and Sakhalin at distances of 352 km, 512 km and 800 km from SP, respectively). Therefore, there are no seismic data connected with this event. Consequently, previous to the current study, the chronology of the eruption has been constructed primarily with satellite data (TERRA, NOAA, MTSAT; SVERT, 2009). Although the Kurils are sparsely populated, they are located within a heavily travelled air corridor linking Europe, North America, and northern Asia. Effective monitoring of Kuril volcanism is therefore imperative for aviation safety (Neal et al., 2009).

Acoustic waves with frequencies ~0.01–20 Hz are named *infrasound*. Here we report atmospheric infrasound observations of the June 2009 SP eruption. Energetic vulcanian and plinian explosions can radiate large-amplitude infrasound directly into the atmosphere (e.g., Garces et al., 2008; Matoza et al., 2009; Fee et al., 2010a, 2010b). In contrast, seismicity (eruption tremor) recorded on dedicated volcano-seismic networks during vulcanian and plinian explosions may result from subsurface processes and/or limited air-ground acoustic–seismic coupling (Matoza, 2009). Consequently, large-amplitude infrasound

* Corresponding author. Tel.: +33169264279.
E-mail address: robin.matoza@cea.fr (R.S. Matoza).

0377-0273/$ – see front matter
doi:10.1016/j.jvolgeores.2010.11.022

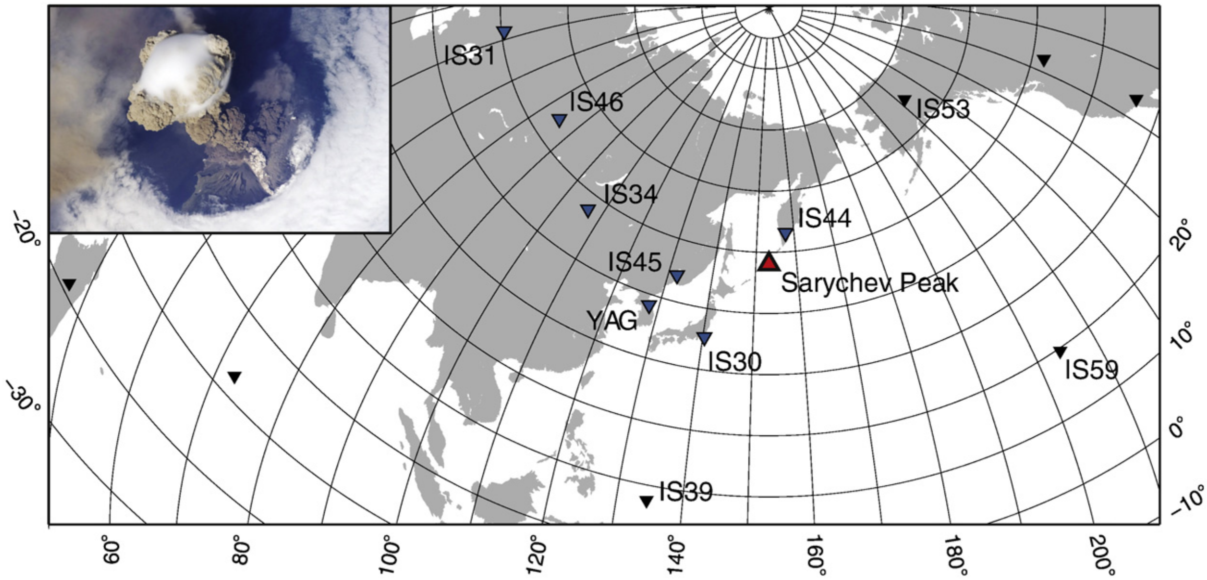

Fig. 1. Map showing location of Sarychev Peak (SP, red triangle), infrasound arrays that recorded signal from SP (blue inverted triangles), and infrasound arrays that did not record signal from SP (black inverted triangles). Signals are observed at long-range to the west of SP corresponding to the stratospheric downwind direction in June 2009. Inset: Astronaut photograph of SP eruption column taken at 22:16 UT 12 June 2009 from the International Space Station (ISS). Image credit: NASA's Earth Observatory.

signals may delineate the exact timing of volcanic explosions, whereas eruption seismicity may be relatively weak or not necessarily correlated with the timing of eruption into the atmosphere.

Infrasound can propagate over large distances in the atmosphere due to low attenuation (Sutherland and Bass, 2004) and due to the formation of waveguides by temperature and wind variations with altitude (e.g., Garces et al., 1998). Whereas remote seismic stations did not record the SP eruption, we report infrasound signals propagating as far as 6433 km from SP in the stratospheric waveguide. However, the details of infrasound propagation in the atmosphere remain a subject of active research (Le Pichon et al., 2010a). For atmospheric studies, volcanoes can represent repetitive sources of infrasound from known and fixed source locations, making them essential ground-truth sources for assessing models of infrasound propagation and atmospheric specifications (Le Pichon et al., 2005). The explosive phase of the eruption sequence at SP lasted for 5–6 days in duration. We use array processing to estimate infrasound wavefront parameters, e.g., backazimuth and trace-velocity (apparent velocity of the wavefront across the array), as a function of time during the eruption sequence. We show that the estimated back-azimuth, trace-velocity and signal frequency content of infrasonic signals from repetitive explosions exhibit systematic variations with time that can be explained by atmospheric variability.

This paper is organized as follows. In Section 2 we describe the sequence of observations at seven infrasound arrays deployed at ranges of ~640–6400 km from SP. We show how these infrasound observations permit the reconstruction of a more detailed eruption chronology (i.e., with a higher temporal resolution) than is possible with satellite data alone. We then highlight some observed signal characteristics resulting from atmospheric propagation and illustrate the effects of atmospheric propagation on infrasound source locations. In Section 3, we model the infrasound propagation using 3D ray-tracing and realistic atmospheric specifications and attempt a source location including atmospheric corrections. We then illustrate with parabolic equation modeling how diffraction and scattering may influence infrasonic propagation from explosive volcanic eruptions. Sections 4 and 5 consist of discussion and conclusions.

2. Observations

2.1. Data

The International Monitoring System (IMS) includes a global network of infrasonic stations designed to detect atmospheric explosions anywhere on the planet (Christie and Campus, 2010). Each infrasound station consists of an array of at least 4 infrasonic sensors with a flat response typically from 0.01 to 8 Hz (sampled at 20 Hz) and a sensitivity of about 0.1 mPa per count. Fig. 1 shows the IMS infrasound stations and an additional station, YAG, operated by the Korea Institute of Geoscience and Mineral Resources (KIGAM), used in this study. Signals from SP were also recorded at other KIGAM infrasound stations, however, we selected one station (YAG) for use in this study since the KIGAM stations fall at similar ranges from SP. IS44 (Kamchatka) is the closest station to SP at a range of 643 km.

Fig. 2 shows the results of applying Progressive MultiChannel Correlation (PMCC) array processing (Cansi, 1995; Le Pichon et al., 2010b) to the infrasound stations labeled in Fig. 1. PMCC estimates wavefront properties of coherent acoustic energy as a function of time at an array by considering correlation time-delays between successive array element triplets (Cansi, 1995). A grid search is performed over successive time windows and frequency bands. A coherent arrival in a particular time window and frequency band is registered as a "pixel". Pixels are then grouped into "families" of pixels sharing common wavefront properties. PMCC processing was performed in 15 log-spaced frequency bands between 0.02 and 9.5 Hz (window length varied from 120 s to 30 s with overlaps 90% of window length). Fig. 2 shows all PMCC pixels coming from an azimuth corresponding to SP $+/-15°$ as viewed from each array (i.e., for each station, we show all PMCC detections that have an azimuth $+/-15°$ of the azimuth of the great-circle path from the station to SP). In order to align the detections in time and facilitate association of the recordings at the various stations, we have applied a time shift to the detections at each array in Fig. 2. The time shift corresponds to the range divided by a constant celerity of 0.33 km/s. Celerity is defined as the total range travelled divided by the propagation time. The celerity of 0.33 km/s